CHAPTER III
EXPERIMENTAL METHODS

3.1 Catalyst Preparation

In this work, two series of Pt-Sn/Al_2O_3 catalysts were investigated. The alumina support was obtained from Degussa Corporation namely, Aluminium Oxide C. The Degussa alumina was fumed and non-porous and had a BET surface area of 90 m^2/g. The alumina consists of mainly the gamma phase and some of it was in the delta phase. There was less than 0.5% HCl present in the alumina. The platinum precursor used was hydrogen hexachloroplatinate (IV) hydrate Aldrich Chemical Company) containing 39.7 wt% platinum. The tin salt was tin (II) chloride (Aldrich Chemical Company) having 61.7 wt% tin. The monometallic platinum catalyst sample was prepared by impregnation of the support with the platinum salt dissolved in acetone as a solvent. The first series of bimetallic samples was prepared by coimpregnation of the support with a solution of metallic precursors in the solvent. This coimpregnated catalyst series has been the subject of extensive characterization (Sachdev, 1989 and Balakrishnan, 1991). The second series was prepared by sequential impregnation with Sn first on the Al_2O_3 support, and followed by Pt, using the same metallic precursors and solvent as given in the coimpregnated series. The nominal platinum loading was maintained constant at 1 wt % in all catalysts. In the coimpregnated series, the nominal tin loading was varied from 0.1-1.0 wt %. In the sequentially impregnated series, the nominal tin loading was varied from 0.6- 5 wt%. After the soaking step, the catalysts were dried at 393 K and then calcined in air at 773 K for 2 hours. After calcination, the catalysts were reduced for 5 h in flowing hydrogen at 673 K.

3.2 Catalyst Characterization

3.2.1 Neutron Activation Analysis

The actual platinum, tin and chlorine contents of the prepared catalysts were quantified by neutron activation analysis at the University of Michigan nuclear reactor lab with the help of the staff at the department of nuclear engineering. The catalyst samples were delivered via pneumatic tube to a location with an average neutron flux rate of 2.13×10^{12} n/cm^2.s and exposed to irradiation for 1 min, followed by single 500-second count of gamma-activity after a 20 minute decay. Calculations of element concentrations were based on comparisons with high-purity single-element standard reference materials.

3.2.2 Chemisorption

Before performing any calculations using the chemisorption results, understanding the nature of chemisorption of the gas on the metallic surface is crucial. One of the important parameters that have to be determined is the chemisorption stoichiometry, which is defined as the number of atoms of gas that are adsorbed on one surface metallic atom. In the case of Pt the following chemisorption stoichiometries have been determined for H_2 and O_2 gas

$$Pt + (1/2)\,H_2 \longrightarrow Pt\text{-}H \quad \text{(H chemisorption, HC)}$$
$$Pt + (1/2)\,O_2 \longrightarrow Pt\text{-}O \quad \text{(O chemisorption, OC)}$$
$$Pt\text{-}O + (3/2)\,H_2 \longrightarrow Pt\text{-}H + H_2O \quad \text{(H titration, HT)}$$
$$2Pt\text{-}H + (3/2)O_2 \longrightarrow 2Pt\text{-}O + H_2O \quad \text{(O titration, OT)}$$

The ratio of chemisorption stoichiometry of Hydrogen Chemisorption : Oxygen Chemisorption : Hydrogen Titration was determined to be 1:1:3.

The dispersion (D) of Pt in supported Pt catalysts has been defined as:

$$D = (N_s/N_t)\ x\ 100 \qquad (3.1)$$

where, D = percentage dispersion

N_s = number of atoms of Pt on the surface

N_t = number of atoms of atom overall in the catalyst

The value of N_t can be obtained from neutron activation analysis and the total weight of sample that was used for the chemisorption experiment. The value of N_t can be also obtained from the saturation chemisorption uptake of the adsorbate used and the chemisorption stoichiometry for the chemisorption of those particular adsorbates on the surface of Pt. The chemisorption average particle sizes, which are also surface average particle sizes are obtained by assuming spherical particle shapes. The average area occupied by one Pt surface atom is assumed to be 0.089 nm^2 (Gruber, 1962). The chemisorption average metal particle size is defined as:

$$d = 6/S\rho \qquad (3.2)$$

where, S = metal surface (area/g metal)

ρ = density of metal

3.2.2.1 Pulse Chemisorption

Prior to pulse chemisorption, the catalyst samples were reduced in purified hydrogen at a flow rate of 15 ml/min for 2 h. at 673 K. The temperature was controlled to ± 1°C by an Omega CN8000 temperature controller. The reduced samples were purged in purified nitrogen at 673 K for 30 min and then cooled to room temperature in nitrogen atmosphere. Gas mixtures of $5\%H_2/N_2$ and $5\%O_2/N_2$ were used as adsorbates. An injection of one of these gas mixtures into a N_2 carrier gas stream flowing at 30 ml/min was made in every 5-minute intervals until no further gas uptake by the catalyst was observed as indicated by constant peak areas of the last few injections. The total amount of adsorption could be calculated by summarizing the gas uptake observed in the series of injections until saturation was reached. A gas chromatograph (HP 5890) with thermal conductivity detector (TCD) was employed to measure both hydrogen and oxygen compositions in the outlet streams.

3.2.2.2 Static Volumetric Chemisorption

The details of the static volumetric chemisorption experiments have been described comprehensively (Balakrishnan, 1991). A catalyst sample was pre-reduced in a hydrogen flow of 15 cc/min at 673K, followed by evacuation. Static reduction with research-grade H_2 was done at 673 K in a partial pressure of 33.3 kPa for 3 h, and followed by evacuation. A second static reduction with hydrogen was carried out at 33.3 kPa at 673 K for 10 h. Finally, hydrogen was removed from the catalyst surface by evacuation at 693 K, followed by cooling of the catalyst sample to ambient temperature under dynamic vacuum. Both H_2 and O_2 adsorption isotherms were then obtained. The first isotherm represented the total H_2 or O_2 uptake at 298 K. The second isotherm was obtained after removing the weakly adsorbed hydrogen or oxygen by evacuation at 298 K for 1 hour.

3.2.3 Temperature Programmed Desorption (TPD) of Methanol

Theory of TPD (Temperature-Programmed Desorption)

The simplest theoretical model describing gas-solid adsorption is the well-known Langmuir adsorption isotherm. This model will be recalled briefly in the case of both nondissociative and dissociative adsorption. The effect of kinetic parameters of the desorption phenomena have been qualitatively visualized by generating sets of theoretical TPD curves through computer simulation (Lemaitre *et al.*, 1984). The experimental variables, such as heating rate and carrier gas flow rate, will also affect the desorption characteristics on the studied surface. Finally, the effect of diffusion limitations needs to be taken into consideration.

A. Nondissociative (First-Order) Adsorption

The adsorption process of a gas (G) on a solid (S) may be considered as a chemical reaction between a gaseous molecule or atom with some adsorption sites (S*) present at the solid surface:

$$S^* + G \leftrightarrow S-G \tag{3.3}$$

The Langmuir model is based on the hypotheses that a fixed number of sites N (F/cm^2) are present on the solid and that the enthalpy of adsorption ΔH_a is independent of the fraction of occupied adsorption sites. It is also assumed that both N and ΔH_a are temperature independent.

If N is the number of sites occupied at given time t, the rate of adsorption is given by

$$\frac{dN}{dt} = pkn_a(N^* - N) - k_d N \tag{3.4}$$

where, N* is the number of sites.

(N*-N) is the number of vacant sites.

p is adsorbate pressure over the solid.

kn_a is the kinetic constant of adsorption.

k_d is the kinetic constant of desorption.

In the case of TPR investigation, the measured quantity is the adsorbate concentration (C) in the carrier gas sweeping the sample. In the case of an ideal reactor, it has to be assumed that no axial or lateral concentration gradient exists. The TPD experiment is normally conducted using a linear heating schedule. The following equations are obtained:

$$C = -\frac{S}{F}\frac{dN}{dt} \tag{3.5}$$

$$C(T) = \frac{SN^*\theta A_d \exp(-E_d/RT)}{F + SN^*(1-\theta)\sigma(RT/2\pi M)^{1/2} A_a \exp(-E_a/RT)} \tag{3.6}$$

$$\frac{d\theta}{dT} = -\frac{F}{S\beta N^*}C(T) \tag{3.7}$$

where, C is the adsorbate concentration in the gas phase (mol/cm^3).

S is the specific surface area of solid (cm^2/g).

F is the specific flow rate of the carrier gas (cm^3 STP/ (s·g)).

β is the heating rate (K/s).

σ is the surface area occupied by one adsorption sites (cm^2/mol).

θ is the surface coverage.

M is the molecular weight of the adsorbate (g/mol).

R is the gas constant (J/ (K· mol)).

T is the absolute temperature (K).

A_d is the entropy factor.

E_a is the activation energy of the adsorption process.

A_a is the frequency factor

E_d is the activation energy of the desorption process.

B. Dissociative (Second-Order) Adsorption

Adsorption of gas molecules on a surface may lead to dissociation of the adsorbate into two or more fragments, which then occupy surface sites. For desorption to take place, these fragments have to recombine. The dissociative adsorption of diatomic molecules such as H_2, or O_2 may be viewed as a chemical reaction with surface sites.

$$2S^* + G_2 \leftrightarrow 2S-G \tag{3.8}$$

The adsorption rate can be expressed by the following equation:

$$\frac{dN}{dt} = pkn_a(N^*-N)^2 - k_dN^2 \tag{3.9}$$

The above equation is second power with respect to the number of unoccupied surface sites, (N*-N), and occupied surface sites, (N), as a consequence of the assumption that each dissociatively adsorbing molecule occupies two surface sites.

The equations representing the TPD features can be described by the following relationship:

$$C(T) = \frac{SN^{*2}\,\theta^{2}\,A_d \exp(-E_d/RT)}{F + SN^{*2}\,(1-\theta)^{2}\,\sigma(RT/2\pi M)^{1/2}\,A_a \exp(-E_a/RT)} \tag{3.10}$$

$$\frac{d\theta}{dT} = -\frac{F}{S\beta N^{*}} C(T) \tag{3.11}$$

C. Diffusion-Controlled Desorption

Up to now, diffusion of the adsorbate in the pores of the solid has not been considered. However, there are instances, especially on supported catalysts, where slow diffusion in the pores might control the rate of adsorption. A general mathematical model of diffusion in the pores of a catalyst is extremely difficult and will therefore not be considered here.

Theory of TPR (Temperature-Programmed Reaction)

Gas-solid reactions can be divided into the following steps: (Lemaitre *et al.*, 1984)

1. Transport of the gaseous reactant from the bulk gaseous phase toward the solid-gas interface (diffusion)
2. Adsorption of reactant on the solid surface
3. Interfacial processes
4. Desorption of the gaseous products from the solid surface
5. Transport of the products away from the solid-gas interface toward the bulk gaseous phase (diffusion).

Each of these steps may control conceivably the overall rate of the process. The sorption (steps 2 and 4) and diffusion steps (steps 1 and 5) have been discussed in the previous section. The present section will therefore focus on step 3.

Extensive reviews of proposed mechanisms for interfacial processes of gas-solid systems have been published in several well-known papers. In this section, the processes most relevant to catalysis studies will be considered. To illustrate the

influence of kinetics and other experimental factors, Lemaitre *et al.* (1984) has developed theoretical TPR curves from selected model mechanisms.

The TPD and TPR techniques can provide very interesting results and help toward a better understanding of the studied system, provided that other information gained from other techniques is available: for instance, a priori knowledge of the chemical nature and of the state of dispersion of the reactive phase.

For this study, the TPD experiments were separated into 2 parts. The first part focused on quantitative determination of the amount of gas desorption by measuring thermal conductivity of the effluent gas. The second part was mass spectrometric identification of the nature of molecular species contributing to each TPD peak.

3.2.3.1 Quantitative TPD Experiments

A catalyst sample weighing 0.05 g was placed into a quartz tube reactor, which was externally heated by a tube furnace. Prior to temperature programmed desorption (TPD), the sample was reduced for 2 h at 673°C with a stream of purified hydrogen at a flow rate of 25 ml/min. After completing the reduction step, the catalyst was cooled down to room temperature by introducing a stream of ultra high purity nitrogen. TPD of methanol experiments were performed using a Micromeritics TPD/TPR 2900 unit. The temperatures of the thermal conductivity detector (TCD), valve and injection loop were maintained at 100°C, 100°C, and 75°C, respectively. UHP nitrogen was selected as carrier gas with 50 ml/min flow rate. The detector current was set at 55 mA. The experimental setup contained three gas lines. The first line served as pretreatment gas line, the second line provided carrier and reference gases, while the third line was used for carrying the solvent vapor to the injection loop. Once the adsorption process was complete, the furnace controller was set to ramp the furnace temperature up to 800°C at a linear ramp rate of 10°C/min. As the temperature increased, surface species began to desorb and the signal of the desorbed species from the thermal conductivity detector was displayed as a function of temperature. Graphically, the TPD/TPR data are represented as peaks in signal versus time plots and temperature versus time plots. The location of peaks on the temperature axis depicts the strength of adsorption. For simple adsorbates that do not undergo decomposition during TPD, the number of

peaks can indicate the number of energetically distinct surface sites. The area under each peak represents the quantity of adsorbed species on a given type of surface sites. The adsorbate used in this study, however, is likely to undergo decomposition at elevated temperatures, and this can lead to additional peaks in the TPD spectrum.

3.2.3.2 Qualitative TPD Experiments

These experiments were performed on 100-250 mg of a prepared catalyst. The catalyst was placed in a 1.2 cm. o.d. tubular quartz reactor. Prior to temperature programmed desorption the catalyst sample was again reduced at 400°C for 2 hours in flowing purified hydrogen. After reduction, the catalyst was flushed with ultra high purity helium at 400°C for 30 min and then cooled down to room temperature in a flow of helium. After that the flow of 20 ml/min helium was switched and sent to a pyrex glass saturator, which contained methyl alcohol at room temperature. The helium stream containing methyl alcohol vapor was passed through the catalyst bed for 30 min. The catalyst bed was purged with flowing helium until there was no longer any trace of methyl alcohol observed by mass spectrometry. Then the reactor was heated up using a linear temperature rise of 40°C/min to 600°C in the flow of 100 ml/min He. The temperature of the furnace was controlled by an OMEGA CN8500 controller and recorded using a computer data acquisition system with LabVIEW software. The effluent gas from the reactor was split using a packless two-way valve (Nupro model SS-BNVCR4). A small portion of the effluent gas was sent into an ultra high vacuum (UHV) system, operating at a base pressure $< 10^{-9}$ torr, through a variable leak value (Varian model 1000). Both valves were heated to avoid condensation of methyl alcohol. A Micromass PC Residual Gas Analyzer (RGA), from VG Quadrupoles, was used for analyzing the gases desorbing from the surface of the catalyst. The RGA was placed in the ultra high vacuum system, which was pumped by a turbomolecular pump (Balzers model TPU 420). The pressure was detected by an ionization gauge tube (Varian). During TPD experiments, the pressure in the UHV chamber was kept at 7×10^{-6} torr.

3.2.4 X-ray Photoelectron Spectroscopy

Electron Spectroscopy for Chemical Analysis (ESCA), also known as X-ray Photoelectron Spectroscopy (XPS) is a surface sensitive technique that can detect changes in relative concentration of surface atoms. It is also used to detect the oxidation states of the elements, which are present on the surface of the sample. XPS has found widespread use in heterogeneous catalysis due to its versatility in studying the surfaces of catalysts (Barr, 1983). The ESCA-PHI 5400 system present in the Electron Microbeam Analysis Laboratory, The University of Michigan, Ann Arbor, USA was used in the XPS work. The XPS apparatus consists of the following subsystems: the vacuum system and associated electronics, the integrated console, the X-ray generator, the analyzer-detector and associated electronics, the computer electronics, the sample manipulation system electronics with sample processing hardware, the optional sputtering system, and an in-situ reactor capable of operating at temperature up to 873 K (Rusch, 1984).

The ESCA process consists of bombarding the sample with monoenergetic photons, usually AlKα (1,486.6 ev) or MgKα (1,253.6 ev), which causes the ejection of electrons from core and valence shells in which the ionization potential, or binding energy, is smaller than the primary photon energy. For solids the binding energy may be calculated from:

$$E_b^f = h\nu - E_{kin} - \phi_{sp} \qquad (3.12)$$

where, E_b^f = the binding energy of the electron in the solid

$h\nu$ = the energy of the exciting radiation

E_{kin} = the measured electron kinetic energy

ϕ_{sp} = the work function of the spectrometer

The superscript f indicates that an electron at rest at Fermi level is assigned zero energy. The number of electrons detected is plotted against the electron kinetic energy to give the photoelectron spectrum. By calculating the binding energy for the different peaks and comparing them with tabulated binding energies elemental identification can be performed.

The experimental protocol initially consisted of taking a small amount of the catalyst sample (prereduced, flowing H_2 for 5 h at 673 K), which was to be analyzed, and pressing it into a thin wafer. Then a small piece of the wafer was placed on the sample holder. Screws were used to hold the sample in place. The sample holder was then placed in a carousel, which was in turn placed inside the sample introduction chamber. The sample introduction chamber was pumped down by a turbomolecular pump. The gate valve between the introduction chamber and the main UHV chamber of the XPS machine was now opened and the sample holder was introduced into the main chamber with the help of a fork and placed in a eight chamber carousel. When the fork was pulled out the gate valve automatically closed. The UHV chamber was pumped by an ion pump and an optional titanium sublimation pump was also present. The vacuum in the UHV chamber was usually better than 1×10^{-8} torr.

Then the position of the sample in the main chamber was adjusted so that the X-rays from the source were focused with maximum efficiency on the sample. Then the X-ray source was turned on. The PHI 5400 XPS machine has a dual anode X-ray source, namely a Mg anode and an Al anode. There are both advantages and disadvantages of using a particular type of source and one should decide on which source to use based on the nature of analysis that has to be performed. For instance, the Al anode can be used to study a larger binding energy range of photoelectron emissions as compared to the Mg anode but the energy resolution is better in the case of the Mg anode hence leading to lesser extent of peak broadening. After the desired X-ray source had been turned on it was ready to collect the XPS spectrum. Initially a survey spectrum was collected which scanned the entire binding energy range and provided a general idea as what elements are present on the surface of the sample. Then a multiplex spectrum was collected in which smaller regions of the spectrum were scanned for longer periods of time so that more details of a particular region of interest were obtained. Electron energy analysis was carried out by a Spherical Capacitor Analyzer, which is controlled by an electronics unit that is completely computerized. A Perkin-Elmer 7500 computer controlling the operation of the machine was used for data collection and manipulation. If depth profiling was required than a sputter ion gun was used. Using this sputter gun, it could raster an

area of 1.5 by 1 nm on the surface of the sample. The gas used for the sputtering experiments was argon.

The in-situ reactor attached to the main XPS chamber was used to reduce the catalyst sample in flowing hydrogen at 673 K before XPS analysis. The reduction step was essential since during the prereduction step, it was exposed to air subsequently, and this could lead to some extent of surface oxidation of the metals, making it necessary to reduce it again before XPS analysis. With the help of the transfer forks the sample holder was transported into the reactor chamber, which was then sealed. Then the gas flow of hydrogen was turned on and the sample was heated to the reduction temperature. After the reduction step the sample was allowed to cool down to room temperature, the gas flow was then turned off, and the chamber was pumped down by a turbomolecular pump, before transporting the sample back to the main UHV chamber for XPS analysis. By this procedure one could obtain reduced catalytic surfaces which had not been exposed to air after the reduction step, and hence one could determine what the oxidation states of the metals were after this reduction pretreatment.

Though the ESCA technique is very versatile, it also suffers from some limitations. One of them is that it allows only macroscopic resolution, and is sensitive to only about 1% of a monolayer. Also there might be sample degradation caused by the photon beam. Another difficulty that is present in XPS analysis is that at times signal overlap might occur, making it necessary to either use regions of the photoelectron spectrum to qualitatively and quantitatively identify the elements, or use software to try to deconvolute the peaks belonging to the elements that overlap. Another problem that occurs while studying supported catalyst samples is that photoelectron peaks are shifted by a few ev from where one would expect them to be present because of static charging. This occurs because as the photoemission process takes place and the atoms loose electrons, there is accumulation of positive charge on the surface of non-conducting specimens. Due to this positive charge the motion of photoelectrons from the specimen is retarded causing their kinetic energy to be lower than what the equation relating kinetic energy and binding energy predicts (Swift *et al.*, 1983).

The three most common methods used to correct for static charging are:

a) Use of an internal standard like the Al 2p photoelectron peak in samples that have Al_2O_3 as the support material, and assuming that this peak lies at the same position irrespective of the nature of the system. Then the shift due to static charging is obtained be calculating the difference in position of the observed Al_2O_3 peak from the actual value. Then this difference is used to calculate the actual position of the photoelectron peaks corresponding to the other elements in the specimen. One problem with this method is that it does not account for metal-support interaction effects.

b) Use the value of a photoelectron peak like the C 1s peak which is produced by adventitious surface layers of carbon to correct for static charging. This is done by obtaining the difference between the observed peak position and an actual value, correcting the other photoelectron peaks using this value. A problem that is encountered when using this method is that literature reports actual values of the C 1s line varying from 284.6 to 285.2 ev.

c) Use a low-energy electron flood gun, which would supply electrons and try to neutralize the positive charge on the insulator surface, hence correcting for the sample charging. This method is also advantageous in another respect that it could decrease peak broadening. By making use of an electron flood gun and then using an internal standard to further correct the peak position, the accuracy in determining the actual peak position is increased.

3.3 Methanol Oxidation Experiment

Figure 3.1 shows the experimental set up for methanol oxidation study. The oxidation of methanol was carried out in a pyrex vertical tube reactor. 0.05-0.1 grams of a catalyst powder was placed between two layers of glass wool. Prior the oxidation, the catalyst sample was pretreated in flowing hydrogen at 673 K for 2 h and purged in helium stream at 673 K for 30 min. Then the catalyst sample was cooled down to the desired reaction temperature that was varied from room temperature up to 373 K. Methanol was vaporized by passing helium through a bubbler containing liquid methanol at 278 K. The methanol-laden helium was then mixed with oxygen and the second helium lines to give gas mixtures having 1,200, 1,000, 770, and 500 ppm of methanol with 21% O_2 and balance with He. The flow rates of gases were controlled by using mass flow controllers (Sierra series 840 Side-Trak). The feed mixture gas was passed upward through the reactor. The total flow rate through the reactor was 260 cm^3min^{-1} giving a space velocity of 20,000 h^{-1}. The catalytic reaction was performed using a continuous flow method at atmospheric pressure. The compositions of feed gas and outlet gas were principally analyzed by a gas chromatograph (Perkin-Elmer, Autosystem XL) equipped with a Flame Ionization Detector (FID) and a Carbopack B/3% SP-1500 column, and with a Thermal Conductivity Detector (TCD) and a 60/80 Carboxen-1000 column. The temperatures of FID and TCD were 393 K and 473 K, respectively. The gas chromatographic separations were carried out isothermally at 333 K.

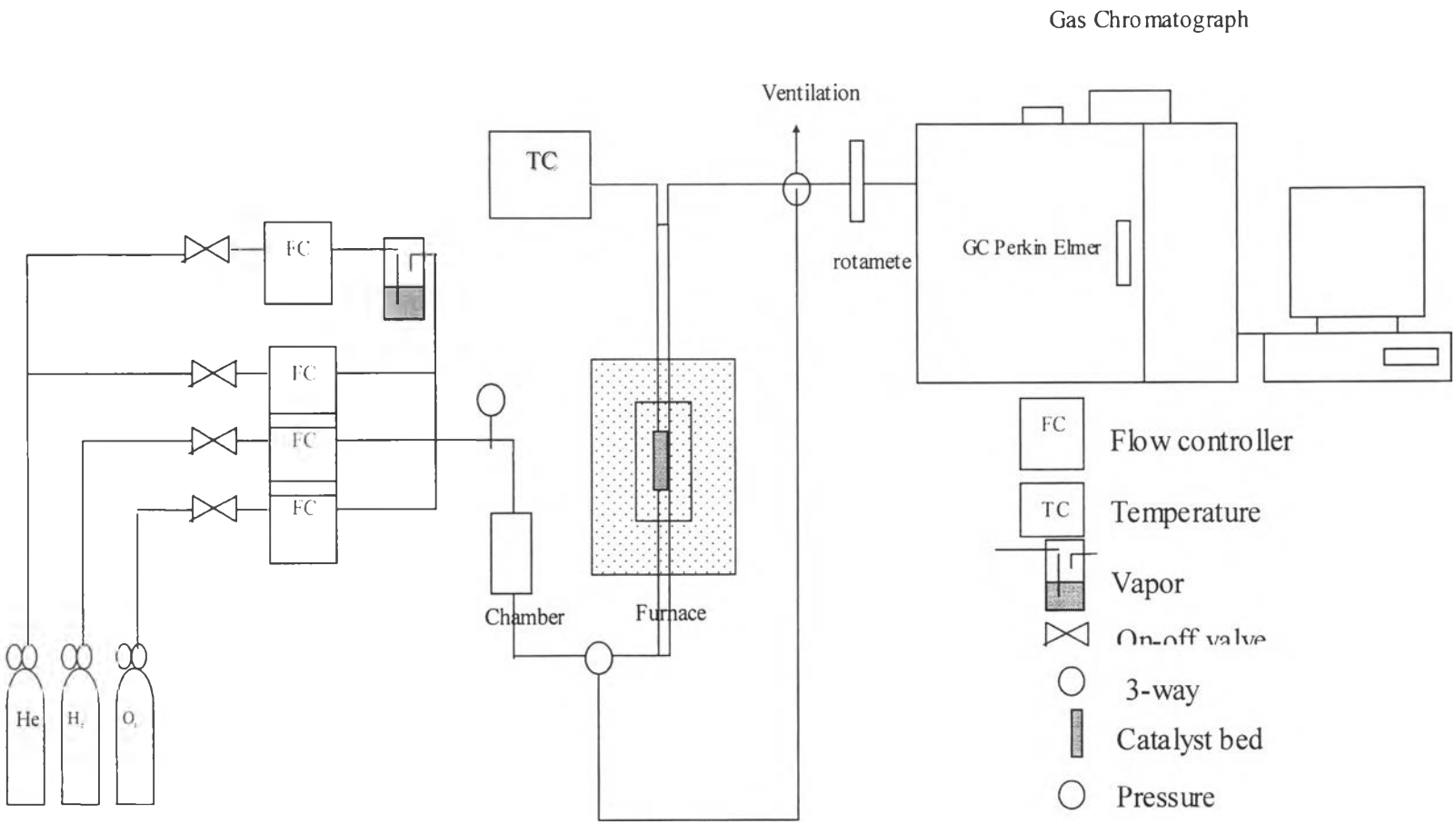

Figure 3.1 Schematic of gas flow methanol oxidation system.